

# Room-temperature optical polarization of nuclear ensembles in diamond

Ran Fischer<sup>1,\*</sup>, Andrey Jarmola<sup>2,3</sup>, Pauli Kehayias<sup>2</sup>, and Dmitry Budker<sup>2,4,+</sup>

1. Department of Physics, Technion – Israel Institute of Technology, Haifa 32000, Israel
2. Department of Physics, University of California, Berkeley, CA 94720-7300, USA
3. Laser Centre, The University of Latvia, Rainis Boulevard 19, 1586 Riga, Latvia
4. Nuclear Science Division, Lawrence Berkeley National Laboratory, Berkeley, CA 94720, USA

We report polarization of a dense ensemble of nuclear spins in diamond at room temperature. The polarization method is based on the transfer of electron spin polarization of negatively charged nitrogen vacancy (NV) color centers to the nuclear spins via the excited-state level anti-crossing (ESLAC) of the center. We demonstrate polarization of 80% of the  $^{14}\text{N}$  nuclear spins related to the NV centers, as well as polarization of 50% of the proximal  $^{13}\text{C}$  nuclear spins. This work may enable polarization of the  $^{13}\text{C}$  in bulk diamond, which is of particular interest to applications of nuclear magnetic resonance, to quantum memories in hybrid quantum devices, and in sensing.

PACS numbers: 61.72.jn, 78.55.Qr, 76.70.Fz

Nuclear spins are a natural choice for applications requiring long relaxation times due to their relatively high immunity to unwanted perturbations from the environment. Among the many applications are magnetic-resonance based bio-sensing [1], various kinds of metrology [1], and quantum computing [4–6]. Specifically, nuclear spins of  $^{13}\text{C}$  (1.1% of natural abundance) are of particular interest to nuclear magnetic resonance (NMR) applications due to the dominant role of carbon in biological systems. Diamond lattice in particular is made up of is pure carbon, while the feeble interaction of the  $^{13}\text{C}$  nuclear spins with the lattice result in long relaxation times [7]. However, thermal polarization of nuclear spins is limited by the Boltzmann factor, which can be extremely small, especially at room temperature, due to the small nuclear magnetic moment. Dynamic nuclear polarization (DNP) enables to achieve higher polarization by transferring the electron-spin polarization to the nuclei. Earlier work on DNP in diamond includes ensemble polarization at cryogenic temperatures [8–11] as well as single-spin polarization at room temperature [12, 13]. Nevertheless, room-temperature polarization of a nuclear *ensemble* has not been demonstrated in diamond until now. Ensemble polarization would be beneficial for obtaining a high signal-to-noise ratio in precision measurements based on nuclear spins and in initializing and manipulating collective quantum memories [14].

Here, we demonstrate polarization of a dense ensemble of nuclear spins in diamond, which comprise approximately  $10^{10}$  spins, by applying the method suggested in Ref. [12] and demonstrated for single nuclear spins of  $^{15}\text{N}$ ,  $^{14}\text{N}$ , and  $^{13}\text{C}$  [12, 13]. This method, applicable at room temperature, is based on the transfer of the polarization of the electron spins of negatively charged nitrogen vacancy (NV) color centers to the nuclear spins at the excited-state level anti-crossing (ESLAC) of the center. In Refs. [12, 13], the method was demonstrated with single centers, while its applicability to ensembles is not trivial due to the local effects such as strain. Nevertheless, this method can be applied to ensembles owing to the averaging of the orbital angular-momentum by strong phonon interactions [14]. We demonstrate a

polarization degree of 80% for the  $^{14}\text{N}$  nuclear spins related to the NV centers, as well as a polarization of about 50% for the proximal  $^{13}\text{C}$  nuclear spins. We study the nuclear polarization dependence on magnetic field strength in the vicinity of the ESLAC, showing a clear effect of the ground-state cross-relaxation of the NV centers and the substitutional-nitrogen (P1) centers.

The negatively charged NV color center in diamond, which is comprised of a substitutional nitrogen atom and a vacancy at an adjacent lattice site, whose negative charge comes from a donor substitutional-nitrogen atom. This center has a spin-triplet ground  $^3\text{A}_2$  and excited  $^3\text{E}$  states connected with an optical transition [16]. The ground state has a zero-field splitting between the  $m_s = 0$  and the  $m_s = \pm 1$  spin sublevels of 2.87 GHz. The  $^3\text{A}_2 \leftrightarrow ^3\text{E}$  transition has a zero-phonon line at 638 nm, and a broadband phonon side-band that spans from 638 nm to about 450 nm in absorption [17]. Optical excitation of the NV center results in optical puming into the  $m_s = 0$  sublevel, due to an intersystem crossing through the singlet  $^1\text{A}$  and  $^1\text{E}$  levels that preferentially transfers the  $m_s = \pm 1$  states from the excited-state  $^3\text{E}$  to the  $m_s = 0$  sublevel in the ground-  $^3\text{A}_2$  state. Due to the difference in fluorescence between the spin-triplet decay  $^3\text{E} \rightarrow ^3\text{A}_2$  and the spin-singlet decay  $^1\text{A} \rightarrow ^1\text{E}$ , the  $m_s = 0$  state fluoresces more than the  $m_s = \pm 1$  sub-states, enabling optical spin read-out. This property enables detection of the allowed spin transitions in the ground-state by optically detected magnetic resonance (ODMR) [18]. Moreover, the hyperfine splitting due to the interaction of the electronic spin of the NV center and the proximal nuclear spins of the  $^{13}\text{C}$  and the  $^{14}\text{N}$  or  $^{15}\text{N}$ , which are a part of the NV center, can be detected in this manner as well.

The polarization process can be understood by examining the excited-state  $^3\text{E}$  Hamiltonian of the NV center (seen in Figure 1 for nuclear spin of  $^{14}\text{N}$ ). At room temperature, the spin-orbit terms and the strain terms are averaged out to zero, due to quenching of the orbital momentum [14], thus the excited state Hamiltonian can be written as [19]

$$(1) \quad H_{es} = D_{es} \left( S_z^2 - \frac{1}{3} S^2 \right) + \gamma_{NV} B \cdot S + \gamma_N B \cdot I + I \cdot A \cdot S.$$

The first term gives rise to the zero-field splitting that separates the electron-spin sub-states  $m_s = 0$  and  $m_s = \pm 1$  by  $D_{es}$ ; the second and third terms are the interaction of the electron and nuclear spins with an external magnetic field, respectively. Here  $\gamma_{NV}$  is the gyromagnetic ratio of the NV center and  $\gamma_N$  is the gyromagnetic ratio of the nuclear spin, typically 3 orders of magnitude smaller than  $\gamma_{NV}$ . The last term is the hyperfine interaction of the nuclear spin and the electron spin of the NV center, where  $A$  is the hyperfine-interaction tensor that has an axial term  $A_{par}$  and a perpendicular term  $A_{perp}$ . It should be noted that the interaction of the strain and the electronic spin term  $E_{es} (S_x^2 - S_y^2)$  is neglected here since it does not change the polarization process significantly. Unless the spin-strain coupling is extremely high, it satisfies  $E_{es} \ll D_{es}$ . For this regime, the term which is proportional to the change in the magnetic field in the anti-crossing is  $E_{es}^2 / 2D_{es}$  [19], which is negligible compared to the hyperfine interaction [19].

Moreover, if the off-axial magnetic-field term (expressed in frequency units) is small compared to the excited-state natural line-width, it can also be neglected. This leaves the hyperfine interaction the only non-secular term in the Hamiltonian, which can be written as:

$$(2) \quad H_{HF} = I \cdot A \cdot S = A_{par} I_z S_z + \frac{A_{perp}}{2} (I_+ S_- + I_- S_+).$$

Near the ESLAC, the mixing of the  $m_s = 0, -1$  states with the  $m_s = +1$  state is low, while the  $m_s = \pm 1$  sub-states are pumped to the  $m_s = 0$  sub-state by optical excitation, we can consider evolution in the subspace with  $m_s = 0, -1$  alone. For the case of the hyperfine interaction with the nuclear spin of  $^{14}\text{N}$ , the Hamiltonian, in the basis of eigenstates of  $S_z, I_z$ , can be written in matrix form, neglecting the  $m_s = +1$  state

$$(3) \quad H_{es} = \begin{pmatrix} \frac{1}{3}D_{es} - \gamma_{NV}B_z + A_{par} & 0 & 0 & 0 & 0 & 0 \\ 0 & \frac{1}{3}D_{es} - \gamma_{NV}B_z & 0 & \frac{A_{perp}}{2} & 0 & 0 \\ 0 & 0 & \frac{1}{3}D_{es} - \gamma_{NV}B_z - A_{par} & 0 & \frac{A_{perp}}{2} & 0 \\ 0 & \frac{A_{perp}}{2} & 0 & -\frac{2}{3}D_{es} & 0 & 0 \\ 0 & 0 & \frac{A_{perp}}{2} & 0 & -\frac{2}{3}D_{es} & 0 \\ 0 & 0 & 0 & 0 & 0 & -\frac{2}{3}D_{es} \end{pmatrix}.$$

The order of the states in the matrix is  $(|m_s, m_l\rangle = |-1, -1\rangle \quad |-1, 0\rangle \quad |-1, +1\rangle \quad |0, -1\rangle \quad |0, 0\rangle \quad |0, +1\rangle)$ , and the magnitudes of coefficients  $D_{es}, A_{par}, A_{perp}$  are:  $D_{es} \approx 1.4 \text{ GHz}$ ,  $A_{perp}, A_{par} \approx \text{tens of MHz}$  [19]. For a magnetic field that corresponds to  $B_z \approx D_{es}/\gamma_{NV} \approx 500 \text{ G}$ , the diagonal terms of  $m_s = -1$  approach the diagonal terms of  $m_s = 0$ , resulting in a strong mixing of the nuclear and electronic spins due to the non-axial hyperfine interaction. In the vicinity of the resulting ESLAC,  $m_s, m_l$  are no longer good quantum numbers, and the  $|m_s = 0, m_l = m\rangle$  and  $|m_s = -1, m_l = m+1\rangle$  states are mixed. The non-axial coefficient of the hyperfine interaction  $A_{perp}$  is on the order of tens of MHz, which is greater than the excited state decay rate. As a result, the mixing of the electronic and nuclear spins in the excited state can take place before the state decays. Since the electron spin of the NV center is optically pumped to  $m_s = 0$  and the  $|m_s = 0, m_l = \max\rangle$  state is not mixed by the hyperfine interaction, the nuclear spin is pumped toward its maximal value. It should be noted that different values of  $A_{par}$  and  $A_{perp}$  depend on the relative location of the nuclear spin with respect to the NV center. This affects the degree of

polarization that can be reached with this method. Therefore, different nuclear-spin species, such as  $^{14}\text{N}$  and  $^{13}\text{C}$ , as well as spins in different positions may exhibit different degree of polarization [20].

An important approximation that we have used in the excited-state Hamiltonian Eq. (1), is neglecting the spin-orbit and strain-orbit terms. In a type-Ib diamond, the strain terms can be large and vary with the location of the center in the sample. This locally splits the excited state, resulting in disappearance of the anti-crossing at 500 G. The quenching of the orbital momentum at room temperature, which allows to neglect these terms was studied previously in different temperatures in emission [15] and in ODMR [21], showing that in room temperature the ESLAC is observed near 500 G, even in type-Ib diamonds, thus enabling the nuclear-polarization process described above.

In our experiments we used a type-Ib diamond with 50 ppm of initial nitrogen concentration that was irradiated with 3 MeV electrons and annealed at 750°C for 2 hours. The NV center concentration after this process is estimated to be on the order of 10 ppm. The inhomogeneously broadened full width half maximum of the ground-state resonance is about 2.5 MHz, so the hyperfine splitting in the ground state due to interaction with  $^{14}\text{N}$  is discernable (2.14 MHz) [22].

The experimental setup is shown in Figure 2. A spherical lens with focal length of  $f = 15$  mm focused a 532 nm laser beam, with a power of 100mW, on the diamond. The fluorescence was collected with the same lens and filtered from the excitation light with a dichroic mirror and a 600 nm long-pass filter, and detected with a photodiode. Microwave (MW) field was applied with a 100  $\mu\text{m}$  diameter copper wire placed near the optical focus on the diamond surface. A magnetic field was applied with a permanent ring magnet and was aligned to less than  $1^\circ$  from the [111] axis. The alignment of the magnetic field with respect to one of the NV centers' orientations is crucial for achieving a high degree of nuclear spin polarization [12]. In magnetic field dependence studies the axial magnetic field was scanned in the range of  $520 \pm 30$  G by controlling the current of a 150 mm diameter copper coil that surrounded the diamond. Note that the polarization process requires only optical excitation that pumps the electronic spin of the NV center, and a proper alignment and magnitude of the magnetic field.

Figure 3 shows a comparison of the ODMR signal contrast for the [111] orientation at low magnetic field and at the ESLAC. Contrast is defined as the fraction change of fluorescence when the microwaves are applied. The ODMR signal at low magnetic field, which is seen at the top trace of Figure 3, exhibits equal contrast on the three hyperfine components of the resonance (unpolarized  $^{14}\text{N}$  nuclei) while the ODMR signal at the ESLAC (bottom trace of Figure 3) exhibits only one dominant resonance with approximately three times the contrast of that at low field. We characterize the nuclear spin polarization degree by analyzing the contrast of ODMR signals. The polarization was calculated to be

$$(4) \quad P = \frac{\sum_i m_i A_i(m_i)}{I \sum_i A_i(m_i)},$$

where  $A_i$  is the relative population of the sub-state  $m_i$ , and  $I$  is the total angular momentum of the state. The relative population was estimated as the ratio of the ODMR-resonance amplitude to the sum of amplitudes of all nuclear sub-states. We estimate that the polarization of the  $^{14}\text{N}$  nuclear spins that

are a part of the NV centers is  $80\pm 5\%$ . We would like to note that the nuclear polarization does not depend on the  $m_s$  state, and the ODMR signal shows similar nuclear polarization for both  $|m_s = 0\rangle \rightarrow |m_s = \pm 1\rangle$  transitions.

Since we deal here with an ensemble of NV centers, some centers have a proximal  $^{13}\text{C}$  nucleus that interacts with the NV center. These NV centers exhibit a double hyperfine splitting – one due to the  $^{14}\text{N}$  nucleus, and one due to the  $^{13}\text{C}$  nucleus [20]:

$$(5) \quad H_{\text{hyperfine}} = I_{^{14}\text{N}} \cdot A_{^{14}\text{N}} \cdot S_{\text{NV}} + I_{^{13}\text{C}} \cdot A_{^{13}\text{C}} \cdot S_{\text{NV}} .$$

The axial coefficient of the hyperfine interaction  $A_{\text{par}}$  with the  $^{14}\text{N}$  nuclear spin in the ground-state is - 2.14 MHz [22], while  $A_{\text{par}}$  of  $^{13}\text{C}$  nuclear spins, which depends on their position with respect to the NV center are between 130 MHz for  $^{13}\text{C}$  in the first shell to about 2.5 MHz for  $^{13}\text{C}$  in the third shell, which is the weakest interaction detected [20]. Since the isotopic abundance of the  $^{13}\text{C}$  is 1.1%, each NV center has a few percent probability to have a  $^{13}\text{C}$  nucleus in each of the relevant positions. Moreover, since the ground-state resonance width is about 2.5 MHz, only interaction with strength greater than about 10 MHz is discernable, meaning that it can be clearly seen above the noise. Therefore, as can be seen in Figure 4, the ODMR signal in low magnetic field, where nuclear polarization is zero, has dominant resonances with a hyperfine splitting due to  $^{14}\text{N}$  and additional resonances, which are marked with arrows in Figure 4, due to the hyperfine interaction with  $^{13}\text{C}$  nuclear spins with strength of 13-14 MHz, which are in turn split due to the  $^{14}\text{N}$  hyperfine interaction.

In an ensemble of NV centers aligned along the magnetic field, the large non-axial hyperfine interaction at the ESLAC results in polarization of both nuclear spin species [20]. This means that the proximal  $^{13}\text{C}$  nuclear spins will be polarized, as well as the  $^{14}\text{N}$  which are part of the NV center. As a result, the ODMR signal of polarized ensemble of nuclear spins of  $^{14}\text{N}$  and proximal  $^{13}\text{C}$ , which can be seen in the bottom trace of Figure 3, is composed of a strong resonance that corresponds to polarization of the  $^{14}\text{N}$  nuclear spin alone, and a weaker resonance, with a contrast of a few percent compared to the strong resonance, that corresponds to polarization of both  $^{14}\text{N}$  and the proximal  $^{13}\text{C}$  nuclear spin. The weaker resonance has a frequency offset from the main resonance equal to half of the  $^{13}\text{C}$  hyperfine splitting. We should note that the  $^{14}\text{N}$  hyperfine interaction [20, 22] has an opposite sign to the  $^{13}\text{C}$  interaction which strength is 13-14 MHz [20]. We estimate that, in this experiment, a polarization of  $50\pm 10\%$  of the discernable proximal  $^{13}\text{C}$  nuclear spins was reached.

The polarization of the proximal  $^{13}\text{C}$  spins can result in polarization of the bulk  $^{13}\text{C}$  by spin diffusion [11]. In Ref. [11] it was estimated that, for a diamond with a concentration of  $\sim 10$  ppm of NV centers concentration with a natural abundance of  $^{13}\text{C}$ , spin diffusion should polarize the bulk  $^{13}\text{C}$  which are found in the optically excited spot at a typical time of tens of seconds. This requires that the bulk  $^{13}\text{C}$  should have a longitudinal spin-relaxation time at room temperature of about a minute. For example, longitudinal spin-relaxation time  $^{13}\text{C}$  in a type-Ib diamond with 10 ppm of nitrogen was measured in Ref. [7] to be more than 1 hour.

In order to find the optimal magnetic-field magnitude for nuclear-spin polarization, we scanned the magnetic field applied parallel to the [111] axis in the vicinity of the ESLAC, while measuring the polarization. We observe that both the fluorescence, and degree of polarization have a dip at 514 G and two additional dips about 15 G above and below (see Figure 5). These dips correspond to cross-relaxation with substitutional nitrogen centers, which reduces the ground-state electron-spin polarization [23], and as a result reduces the nuclear polarization. Apart from these dips the polarization degree is almost independent of the magnetic field in this range. Therefore, the polarization method should be applied in a magnetic field, avoiding the field values corresponding to the dips. If it is necessary to work at one of these field values, maintaining the same degree of nuclear polarization may require higher optical pumping rate.

We have demonstrated a high degree of polarization of a dense ensemble of nuclear spins associated with NV centers in an HPHT diamond at room temperature. The polarization method is based on hyperfine interaction at the ESLAC, and was applied to proximal  $^{13}\text{C}$  as well as the  $^{14}\text{N}$  nuclear spins within the centers. We estimate that a polarization degree of 50% of the discernable proximal  $^{13}\text{C}$  nuclear spins and a polarization degree of 80% of the  $^{14}\text{N}$  nuclear spins was achieved. We demonstrate that when working at room temperature, the interaction with phonons in the excited state of the NV center contributes to averaging of the orbital momentum, enabling the polarization even for diamond with high and inhomogeneous strain.

The dependence of the degree of polarization of the  $^{14}\text{N}$  nuclear spins on the magnetic field in the vicinity of the ESLAC was studied. Cross-relaxation of the NV center with substitutional nitrogen decreases the center's electron polarization, and thus, the nuclear-spin polarization as well. We expect that the decrease in polarization due to cross relaxation can be minimized by increasing the pumping rate, i.e., by increasing the pump intensity.

We envision the following applications of this work. First, the polarization of the proximal  $^{13}\text{C}$  nuclear spins may enable polarization, by spin diffusion, of the  $^{13}\text{C}$  in the bulk of the diamond crystal. The bulk polarization may be especially high for  $^{13}\text{C}$  enriched diamonds, which have a strong dipolar coupling between neighboring  $^{13}\text{C}$  nuclear spins, compared to an isotopically natural diamond. Second, for a diamond with low nitrogen content, a high polarization degree of the proximal  $^{13}\text{C}$  nuclear spins may decrease the coherence decay rate of the ground state in the NV center which is mainly caused by randomly polarized  $^{13}\text{C}$  nuclear spins.

The authors thank M. Ledbetter, V. Acosta, N. Manson, P. Hemmer, M. Doherty and D. English for useful discussions. This work has been supported in part by the AFOSR/DARPA QuASAR program, by IMOD, and by the NATO SFP program. R.F. gratefully acknowledges support from DDRND. A.J. gratefully acknowledges support from the ERAF project No.2010/0242/2DP/2.1.1.1.0/10/APIA/VIAA/036. P.K. gratefully acknowledges support from the DOE SCGF.

\* [rfischer@techunix.technion.ac.il](mailto:rfischer@techunix.technion.ac.il)

+ [budker@berkeley.edu](mailto:budker@berkeley.edu)

Figures:

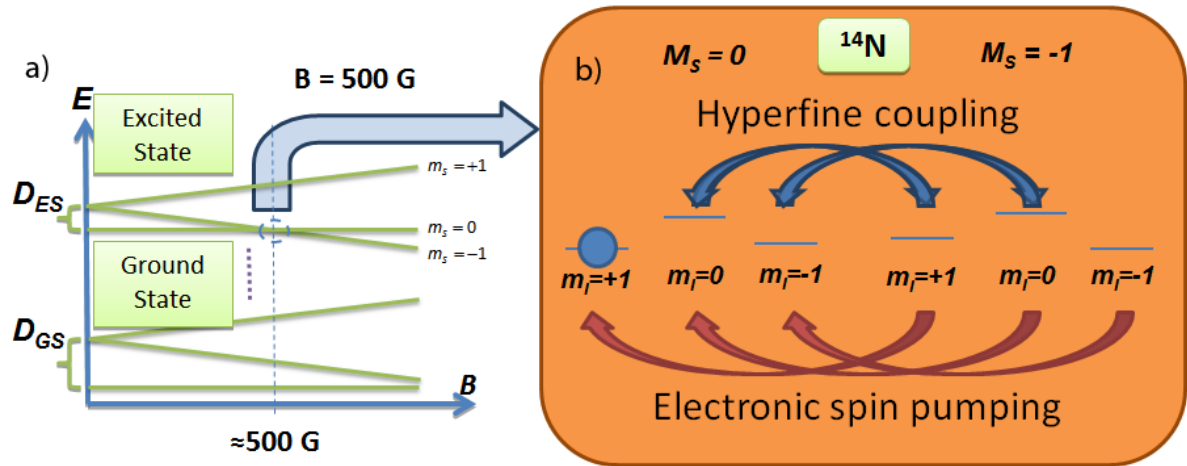


Figure 1 - Nuclear-spin polarization process of the  $^{14}\text{N}$  nuclear spin. a) Energy diagram of the triplet levels of the NV center at room temperature as a function of the magnitude of an axial magnetic field. The ESLAC of the spin-states  $m_s = 0$  and  $m_s = -1$  can be seen in a field of  $\approx 500$  G. b) The hyperfine splitting of the ground state due to interaction with  $^{14}\text{N}$ . The blue arrows symbolize coupling at the ESLAC between the electronic-spin of the NV center and the nuclear spin of the  $^{14}\text{N}$ , while the red arrows symbolize the electronic spin pumping toward  $m_s = 0$ , due to the inter-system crossing. The blue circle represents the state that the system is pumped into and cannot be affected by  $A_{\text{perp}}$ .

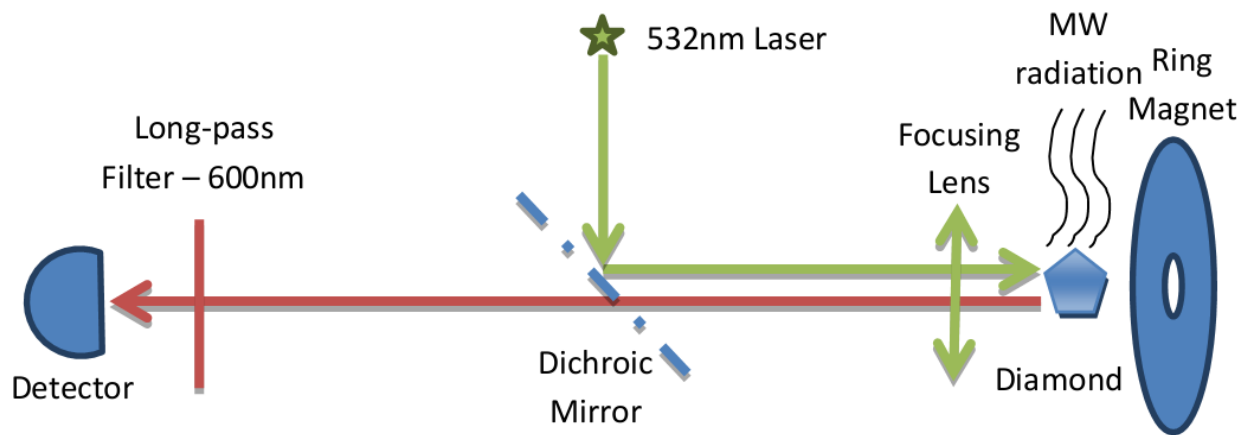


Figure 2 - Experimental setup. The magnetic field is applied axially with respect to the face of the diamond with a permanent ring magnet. The lens focuses the excitation 532nm laser, and collects the fluorescence emitted from the diamond. The long-pass filter blocks wavelengths below 600nm.

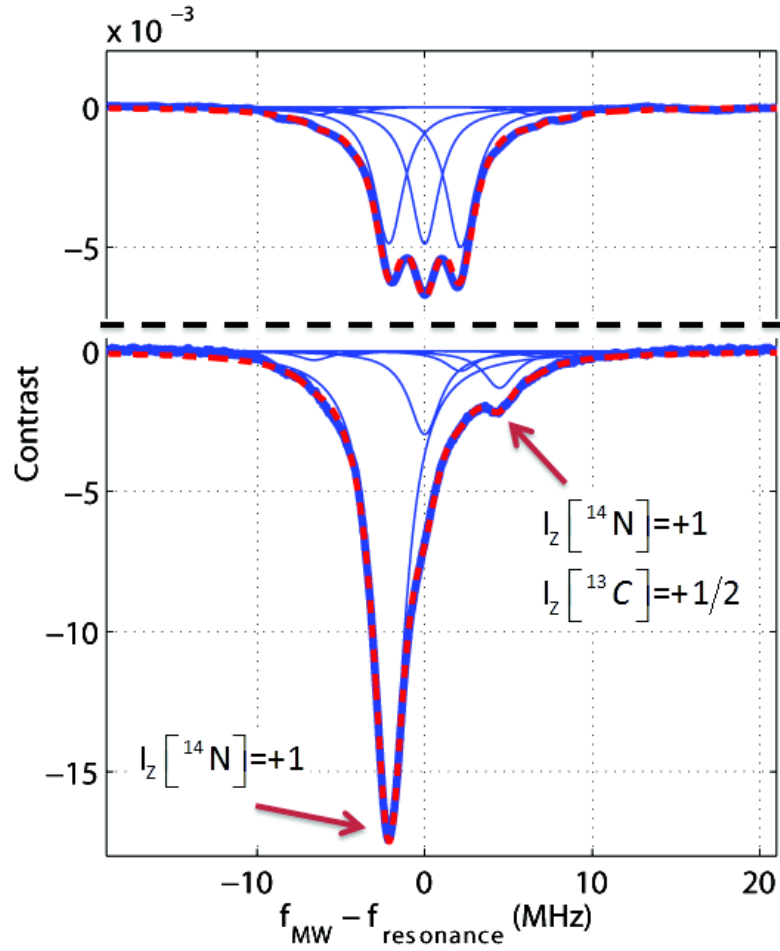


Figure 3 – Comparison of ODMR signal's contrast of the [111] orientation in a low magnetic field and at the ESLAC. Top figure: ODMR signal at low magnetic field. Bottom figure: ODMR signal at the ESLAC. Thick full curve correspond to the experimental results, thick dashed curve correspond to the fitted multiple resonances. Narrow curves correspond to the fitted individual resonances. The high peak corresponds to the  $(m_s = 0, I_z^{14\text{N}} = +1 \rightarrow m_s = +1, I_z^{14\text{N}} = +1)$  transition. The low peak corresponds to  $(m_s = 0, I_z^{14\text{N}} = +1, I_z^{13\text{C}} = +1/2 \rightarrow m_s = +1, I_z^{14\text{N}} = +1, I_z^{13\text{C}} = +1/2)$  transition, and it is due to hyperfine interaction with  $^{14}\text{N}$  and  $^{13}\text{C}$  nuclear spins. Top figure:  $f_{\text{resonance}} = 2.8$  GHz. Bottom figure:  $f_{\text{resonance}} = 4.25$  GHz.



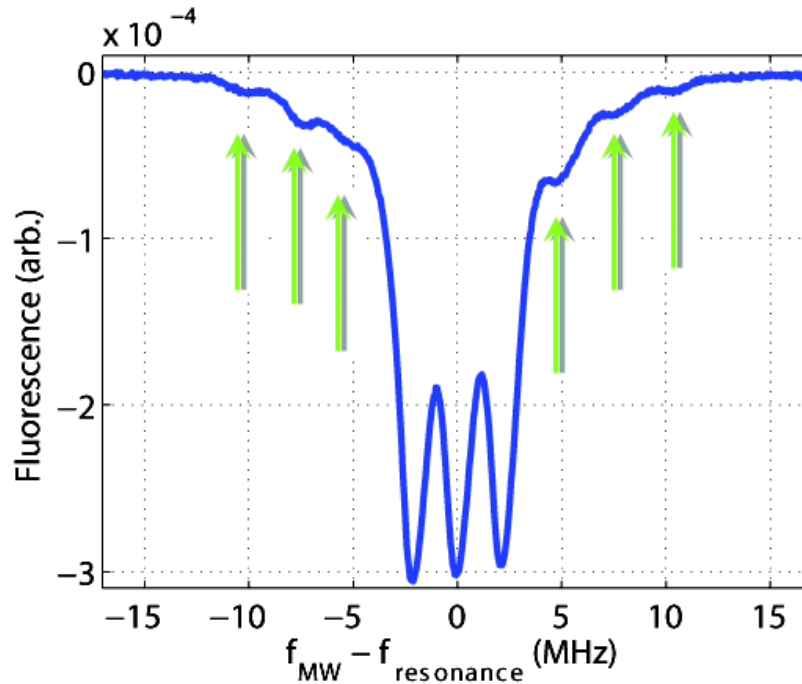


Figure 4 - ODMR signal at low axial magnetic field. The arrows show the hyperfine splitting due to interaction with  $^{13}\text{C}$  in the sites at the third shell which gives interaction strength, stronger than 8 MHz [20]. This splitting is also further split by  $^{14}\text{N}$  hyperfine interaction. This ODMR spectrum was taken with a CVD diamond with  $\sim 0.5$  ppm of nitrogen, which has a smaller inhomogeneous broadening.  $f_{\text{resonance}} = 2.77$  GHz.

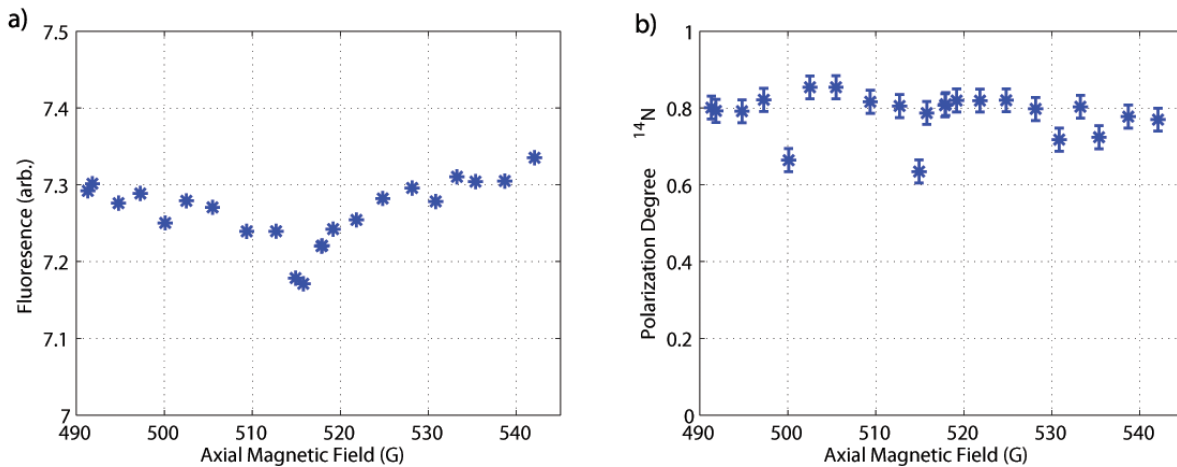


Figure 5 – a) Fluorescence versus magnetic field along the [111] axis. b) Polarization degree of the  $^{14}\text{N}$  nuclear spins within the NV centers aligned with the [111] axis as a function of axial magnetic field.

#### References:

- [1] L. Schroder et al., "Molecular Imaging Using a Targeted Magnetic Resonance Hyperpolarized Biosensor", Science Vol. 314, 446 (2006).
- [2] K. F. Woodman et al., "The Nuclear Magnetic Resonance Gyroscope: a Review", Journal of Navigation 40, 366 (1987).

- [3] T. W. Kornack et al., "Nuclear Spin Gyroscope Based on an Atomic Comagnetometer", *Phys. Rev. Lett.* 95, 230801 (2005).
- [4] L. M. K. Vandersypen, I. L. Chuang, "NMR Techniques for Quantum Control and Computation", *Rev. Mod. Phys.* 76, 1037 (2004).
- [5] J. J. L. Morton et al., "Solid-State Quantum Memory Using the  $^{31}\text{P}$  Nuclear Spin", *Nature* Vol. 455, 1085 (2008).
- [6] M. V. Gurudev Dutt et al., "Quantum Register Based on Individual Electronic and Nuclear Spin Qubits in Diamond", *Science* Vol. 316, 1312 (2007).
- [7] C. J. Terblanche et al., " $^{13}\text{C}$  Spin-Lattice Relaxation in Natural Diamond: Zeeman Relaxation at 4.7 T and 300 K Due to Fixed Paramagnetic Nitrogen Defects", *Solid State Nucl. Magn. Reson.* 20, 1 (2001).
- [8] E. C. Reynhardt and G. L. High, "Dynamic Nuclear Polarization of Diamond. I. Solid State and Thermal Mixing Effects", *J. Chem Phys.* 109, 4090 (1998).
- [9] E. C. Reynhardt and G. L. High, "Dynamic Nuclear Polarization of Diamond. II. Nuclear Orientation via Electron Spin-Locking", *J. Chem Phys.* 109, 4100 (1998).
- [10] E. C. Reynhardt and G. L. High, "Dynamic Nuclear Polarization of Diamond. III. Paramagnetic Electron Relaxation Times from Enhanced  $^{13}\text{C}$  Nuclear Magnetic Resonance Signals", *J. Chem Phys.* 113, 744 (2000).
- [11] J. King et al. "Optical Polarization of  $^{13}\text{C}$  Nuclei in Diamond Through Nitrogen-Vacancy Centers", *Phys. Rev. B* 81, 073201 (2010).
- [12] V. Jacques et al., "Dynamic Polarization of Single Nuclear Spins by Optical Pumping of Nitrogen-Vacancy Color Centers in Diamond at Room Temperature", *Phys. Rev. Lett.* 102, 057403 (2009).
- [13] B. Smeltzer et al., "Robust Control of Individual Nuclear Spins in Diamond", *Phys. Rev. A* 80, 050302 (2009).
- [14] D. R. McCamey et al., "Electronic Spin Storage in an Electrically Readable Nuclear Spin Memory with a Lifetime  $> 100$  Seconds", *Science* Vol. 330, 1652 (2010).
- [15] L. J. Rogers et al., "Time-Averaging within the Excited State of the Nitrogen-Vacancy Centre in Diamond", *New J. Phys.* 11, 063007 (2009).
- [16] N. B. Manson et al., "Nitrogen-Vacancy Center in Diamond: Model of the Electronic Structure and Associated Dynamics", *Phys. Rev. B* 74, 104303 (2006).
- [17] V. M. Acosta et al., "Diamonds with a High Density of Nitrogen-Vacancy Centers for Magnetometry Applications", *Phys. Rev. B* 80, 115202 (2009).
- [18] A. Gruber et al., "Scanning Confocal Optical Microscopy and Magnetic Resonance in Single Defect Centers", *Science* Vol. 276, 2012 (1997).
- [19] G. D. Fuchs et al., "Excited-State Spectroscopy Using Single Spin Manipulation in Diamond", *Phys. Rev. Lett.* 101, 117601 (2008).
- [20] B. Smeltzer et al., " $^{13}\text{C}$  Hyperfine Interactions in the Nitrogen-Vacancy Centre in Diamond", *New J. Phys.* 13, 025021 (2011).
- [21] A. Batalov et al., "Low Temperature Studies of the Excited-State Structure of Negatively Charged Nitrogen Vacancy Color Center in Diamond", *Phys. Rev. Lett.* 102, 195506 (2009).
- [22] S. Felton et al., "Hyperfine Interaction in the Ground-state of the Negatively Charged Nitrogen Vacancy Center in Diamond", *Phys. Rev. B* 79, 075203 (2009).

[23]S. Armstrong et al., "NV-NV Electron-Electron Spin and NV-N<sub>s</sub> Electron-Electron and Electron-Nuclear Spin Interaction in Diamond", Physics Procedia 3, 1569 (2010).